Auger transition rates and fluorescence yields for the double-K-hole state

Mau Hsiung Chen
High Temperature Physics Division, Lawrence Livermore National Laboratory, University of California, Livermore, California 94550
(Received 8 February 1991)

Auger and radiative transition rates and fluorescence yields for the double-K-hole state have been calculated for five elements with $10 \leq Z \leq 36$ using the multiconfiguration Dirac-Fock method. The Auger and x-ray energies are found to shift to higher energies by 68–269 and 100–388 eV, respectively, due to the presence of the K-shell spectator vacancy. For low-Z elements, the transition rates per K hole for the double-K-hole state are much larger than the corresponding rates for the single-K-hole state. As Z increases to higher values, the differences in transition rates diminish. K-shell fluorescence yields for the double-K-hole state compared to the results for the single-K-hole state are found to increase by 33% at $Z=10$ but by only 2.6% at $Z=36$.

I. INTRODUCTION

The radiative deexcitation of the double-K-hole state [$1s^2$] giving rise to the K x-ray hypersatellites has received much attention [1–4] in the past decade. Accurate measurements of hypersatellite energy shift constitute a very sensitive test of magnetic and retardation effects in atoms [3]. Although the x-ray decay of the double-K-vacancy state has been thoroughly studied, the information on the Auger decay and fluorescence yield are rather scarce. To my knowledge, there exists only one calculation on the K-shell fluorescence yield for the double-K-hole state of fluorine ions [5]. Furthermore, in the analysis of experiment on double-K-shell ionization in the electron-capture decay the fluorescence yield of the double-K-vacancy state is assumed to be the same as the value for the single-K-hole state [6,7]. In view of the long-standing discrepancies between theory and experiment for the double-ionization probability P_{KK} in the electron-capture decay [6–9], it is highly desirable to calculate the fluorescence yield for the double-K-hole state and to assess its impact on the experimental determination of P_{KK}. In this work, we report on the calculation of Auger and radiative transition rates and fluorescence yields for the double-K-hole state using the multiconfiguration Dirac-Fock (MCDF) method [10,1]. The calculations were carried out for five ions with $10 \leq Z \leq 36$ in intermediate coupling with configuration interaction including Breit interaction and quantum electrodynamic corrections. In this work, the subshell symbol enclosed by brackets (e.g., [$1s2p$], [KLM]) is used to denote the hole state.

II. THEORETICAL METHOD

Relativistic calculation of Auger and radiative transition rates based on the MCDF model has been described in detail in Ref. [11]. Here, we only outline the essential points. The Auger transition probability is calculated from perturbation theory [12]. The transition rate in the frozen-orbital approximation is given by

$$T=\frac{2\pi}{\hbar}\left|\left\langle \Psi_f \left| \sum_{\substack{\alpha,\beta \\ \alpha<\beta}} V_{\alpha\beta} \right| \right\rangle\right|^2 \rho(\varepsilon) \ . \tag{1}$$

Here, ψ_i and ψ_f are the antisymmetrized many-electron wave functions of the initial bound state and final continuum state of the ion, respectively; $\rho(\varepsilon)$ is the energy density of final states, and $V_{\alpha\beta}$ is the two-electron interaction operator which is taken to be the sum of the Coulomb and generalized Breit operators [13] in the present work.

In the MCDF model, an atomic-state function for a state i with total angular momentum JM can be expanded in terms of configuration-state functions (CSF), which are constructed by taking linear combinations of Slater determinants of the Dirac orbitals:

$$\psi_i(JM)=\sum_{\lambda=1}^{n} C_{i\lambda}\phi(\Gamma_\lambda JM) \ , \tag{2}$$

where n is the number of CSF's included in the expansion, and $C_{i\lambda}$ are the mixing coefficients for state i.

The Auger matrix elements can be expressed in terms of the CSF basis. The matrix element between two CSF's can be separated into angular parts multiplied by radial integrals by using the general angular-momentum package in the MCDF code [10].

In the MCDF model, the relativistic transition probability for a discrete transition $i \rightarrow f$ in a multipole expansion is given in perturbation theory by [11,14]

$$W_{fi}=\frac{1}{2J_i+1} \times \sum_L \frac{2\pi}{2L+1} \left| \sum_{\alpha=1}^{n_i} \sum_{\beta=1}^{n_f} C_{i\alpha} C_{f\beta} \sum_{p,q} d_{pq}^{L}(\beta,\alpha) \times \langle p \| T_L \| q \rangle \right|^2 . \tag{3}$$

Here, the one-electron matrix elements $\langle p \| T_L \| q \rangle$ are given by Grant [14]. The angular factor $d_{pq}^{L}(\beta,\alpha)$ that depends on the configuration-state functions can be calculated using angular-momentum subroutines in the MCDF code [10].

TABLE I. *KLL* Auger energy (in eV) for the double-*K*-vacancy state.

Final state	Atomic number 10	18	30	36
$[1s2s^2]\,^2S_{1/2}$	812.6	2640.3	7432.2	10 672.8
$[1s2s2p]\,^2P^{(+)}_{1/2}$	836.9	2697.5	7547.0	10 820.2
$[1s2s2p]\,^2P^{(+)}_{3/2}$	837.0	2698.8	7560.0	10 845.6
$[1s2s2p]\,^2P^{(-)}_{1/2}$	844.1	2710.6	7578.8	10 869.4
$[1s2s2p]\,^2P^{(-)}_{3/2}$	844.1	2711.3	7584.2	10 887.4
$[1s2s2p]\,^4P_{1/2}$	854.6	2730.7	7607.0	10 906.9
$[1s2s2p]\,^4P_{3/2}$	854.7	2731.9	7618.5	10 928.2
$[1s2s2p]\,^4P_{5/2}$	854.8	2733.5	7630.6	10 949.2
$[1s2p^2]\,^2S_{1/2}$	868.8	2767.4	7685.0	10 998.2
$[1s2p^2]\,^2P_{1/2}$	871.4	2773.1	7716.9	11 064.0
$[1s2p^2]\,^2P_{3/2}$	871.5	2773.9	7712.2	11 055.3
$[1s2p^2]\,^2D_{5/2}$	872.4	2776.9	7721.3	11 068.9
$[1s2p^2]\,^2D_{3/2}$	872.4	2777.1	7730.2	11 082.0
$[1s2p^2]\,^4P_{1/2}$	878.7	2789.1	7745.9	11 116.9
$[1s2p^2]\,^4P_{3/2}$	878.8	2789.9	7748.7	11 121.7
$[1s2p^2]\,^4P_{5/2}$	878.9	2791.8	7764.1	11 144.6

The energies and wave functions for the initial double-*K*-hole state were calculated in a single-configuration approximation. The energies and wave functions for the final ionic states were evaluated in intermediate coupling with configuration interaction using the MCDF model in an average-level scheme (MCDF-AL) [10]. In the MCDF-AL calculations, the orbital wave functions are obtained by minimizing the averaged energy of all the levels with equal weight. For the final triple-hole state after Auger decay, all the states from [*KLL*] and [*KLM*] triple-vacancy configurations were included in the same calculation (e.g., there are 51 and 82 states for Ar and Kr, respectively). The basis set for the final two-hole state in x-ray emission includes all possible states from $[1s2p]$, $[1s3p]$, and $[1s4p]$ configurations. The mixing coefficients $C_{i\lambda}$ [Eq. (2)] were determined by diagonalizing the energy matrix which includes Coulomb and transverse Breit interactions and quantum electrodynamic corrections [10,15]. The transition energies were obtained by taking the differences between the separately calculated total energies for the initial and final ionic states. In the calculations of the transition rates, the corrections due to the nonorthogonality in wave functions were neglected. The Auger transitions leading to [*KLN*]/[*KMM*], [*KMN*], and [*KNN*] final states contribute less than 3% to the total [*KK*] level width. These *jj* configuration-average rates were calculated using the Dirac-Hartree-Slater model [12]. To facilitate the comparison between single- and double-*K*-hole states, the energies and transition rates for the single-*K*-hole state were also calculated using the same procedure employed for the double-*K*-hole state.

TABLE II. *KLL* Auger transition rate (in $\sec^{-1}$) for the double-*K*-vacancy state. The numbers in brackets are powers of 10.

Final state	Atomic number 10	18	30	36
$[1s2s^2]\,^2S_{1/2}$	7.15[13]	1.10[14]	1.51[14]	1.77[14]
$[1s2s2p]\,^2P^{(+)}_{1/2}$	1.08[4]	1.69[14]	2.21[14]	2.43[14]
$[1s2s2p]\,^2P^{(+)}_{3/2}$	2.12[14]	3.04[14]	2.70[14]	1.83[14]
$[1s2s2p]\,^2P^{(-)}_{1/2}$	1.59[12]	3.72[12]	6.67[11]	3.86[11]
$[1s2s2p]\,^2P^{(-)}_{3/2}$	3.39[12]	2.19[13]	1.08[14]	2.08[14]
$[1s2s2p]\,^4P_{1/2}$	5.67[9]	1.73[11]	3.98[12]	1.18[13]
$[1s2s2p]\,^4P_{3/2}$	7.41[9]	3.15[11]	5.46[12]	1.07[13]
$[1s2s2p]\,^4P_{5/2}$	3.38[8]	6.00[9]	5.84[10]	1.28[11]
$[1s2p^2]\,^2S_{1/2}$	8.43[13]	1.20[14]	8.87[13]	8.19[13]
$[1s2p^2]\,^2P_{1/2}$	9.51[10]	1.00[13]	2.45[13]	7.12[12]
$[1s2p^2]\,^2P_{3/2}$	2.44[12]	9.23[13]	3.18[14]	3.68[14]
$[1s2p^2]\,^2D_{5/2}$	4.45[4]	7.10[14]	7.56[14]	7.26[14]
$[1s2p^2]\,^2D_{3/2}$	2.95[14]	3.78[14]	1.49[14]	5.11[13]
$[1s2p^2]\,^4P_{1/2}$	1.91[10]	1.50[12]	3.85[13]	6.62[13]
$[1s2p^2]\,^4P_{3/2}$	2.66[10]	1.67[12]	7.69[13]	1.39[14]
$[1s2p^2]\,^4P_{5/2}$	7.15[10]	5.88[12]	8.56[13]	1.49[14]

TABLE III. X-ray energy (in eV) for the double-K-vacancy state.

Final state	Atomic number 10	18	30	36
$[1s2p]\,^3P_1$	947.7	3140.5	8953.2	13 028.7
$[1s2p]\,^1P_1$	943.4	3130.5	8926.8	12 975.1
$[1s3p]\,^3P_1$		3415.9	9964.2	14 600.5
$[1s3p]\,^1P_1$		3414.8	9960.8	14 592.3

TABLE IV. X-ray transition rate (in $\sec^{-1}$) for the double-K-vacancy state. The numbers in brackets are powers of 10.

Final state	Atomic number 10	18	30	36
$[1s2p]\,^3P_1$	6.30[9]	4.30[12]	7.20[14]	2.39[15]
$[1s2p]\,^1P_1$	3.09[13]	3.07[14]	1.83[15]	2.97[15]
$[1s3p]\,^3P_1$		2.87[11]	8.92[13]	3.49[14]
$[1s3p]\,^1P_1$		3.31[13]	2.34[14]	4.06[14]

TABLE V. Auger width Γ_A, radiative width Γ_R, and fluorescence yield ω for the double-K-vacancy state. All widths are in eV.

Z	Γ_A	Γ_R	ω
10	0.804	0.0204	0.0247
18	1.458	0.226	0.135
24	1.696	0.758	0.309
30	1.860	1.894	0.505
36	2.112	4.074	0.659

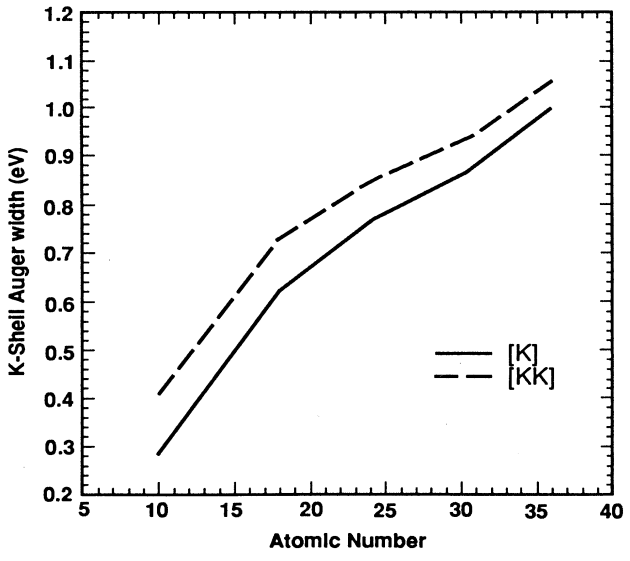

FIG. 1. Auger width per K hole from the present MCDF calculations as functions of atomic number. The solid curve shows the results for the single-K-hole state. The dashed curve displays the values for the double-K-hole state.

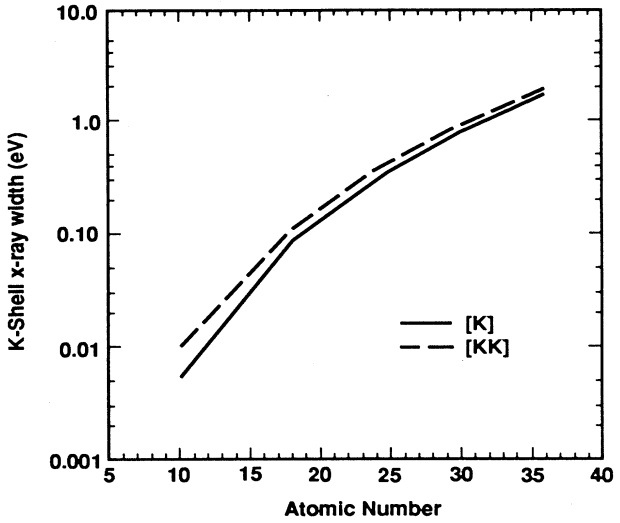

FIG. 2. X-ray width per K hole from the present MCDF calculations as functions of atomic number. The symbols are the same as in Fig. 1.

III. RESULTS AND DISCUSSION

The theoretical KLL Auger energies and transition rates for the double-K-hole state from the MCDF calculations are listed in Tables I and II. The notations $^2P_J^{(+)}$ and $^2P_J^{(-)}$ in Tables I and II represent the higher- and lower-energy states of the ^2P_J states. The electric-dipole transition rates were calculated in length gauge [14]. The results for x-ray energies and transition rates are listed in Tables III and IV. In Table V, the total Auger and radiative widths and fluorescence yields are shown.

The Auger energies for the double-K-hole state increase by 68 and 269 eV for Ne and Kr, respectively. The hypersatellite shifts from the present MCDF calcula-

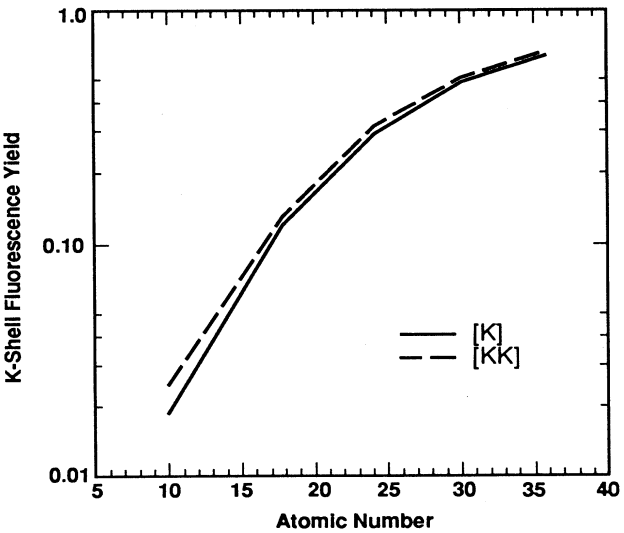

FIG. 3. K-shell fluorescence yield from the present MCDF calculations as functions of atomic number. The symbols are the same as in Fig. 1.

tions agree with the results from the previous Dirac-Hartree-Slater (DHS) intermediate coupling calculations [3] to better than 0.5 eV. The hypersatellite transition rates from this work are larger than the values from the DHS model [3] by 13% and 5.3% for Ar and Kr, respectively.

The total K-shell Auger and radiative widths per K hole for single- and double-K-hole states are compared in Figs. 1 and 2. At $Z=10$, the Auger width per K hole for the double-K-vacancy state is larger than the corresponding value for the single K-hole state by 42%, and the increase reduces to only 6% at $Z=36$. On the other hand, the x-ray width per K hole for the double-K-hole state increases by 89% and 14% at $Z=10$ and 36, respectively, when compared to the corresponding value for the single-K-hole state (Fig. 2).

The K-shell fluorescence yields for the single- and double-K-hole states are displayed in Fig. 3. With the extra spectator K-shell vacancy, the K-shell fluorescence yield increases by 33% at $Z=10$. This rise in fluorescence yield becomes progressively smaller as Z increases. At $Z=36$, the difference in the fluorescence yields between single- and double-K-hole states is only 2.6%. Hence, it is a rather good approximation to assume that the fluorescence yield of the double-K-hole state is the same as the fluorescence yield of the single-K-hole state for $Z \geq 25$.

In summary, we have calculated the K-shell Auger rate, radiative transition rates, and fluorescence yields for the double-K-vacancy state for five elements with $10 \leq Z \leq 36$ using the MCDF method. For the low-Z elements, the transition rates for the double-K-hole state are significantly larger than the corresponding rates for the single-K-hole state. The increase is much reduced for the mid- and high-Z elements. In addition, the increase in radiative transition rate is much larger than the increase in Auger rate. This results in a significant rise in fluorescence yield for the low-Z elements. However, the differences in fluorescence yield between single- and double-K-hole states diminish as Z increases to higher values. Hence, the assumption that the double-K-hole state has the same fluorescence yield as the single-K-hole state contributes very little to the discrepancies between theory and experiment in the double-K-shell ionization in the electron-capture process.

ACKNOWLEDGMENTS

The author would like to thank B. Crasemann for very helpful discussions. This work was performed under the auspices of the U.S. Department of Energy by the Lawrence Livermore National Laboratory under Contract No. W-7405-ENG-48.

[1] J. P. Briand, P. Chevallier, M. Tavernier, and J. P. Rozet, Phys. Rev. Lett. **27**, 777 (1971).
[2] T. Aberg, J. P. Briand, P. Chevallier, A. Chetioui, and J. P. Rozet, J. Phys. B **9**, 2815 (1976).
[3] M. H. Chen, B. Crasemann, and H. Mark, Phys. Rev. A **25**, 391 (1982).
[4] V. Horvat, K. Ilakovac, M. Veskovic, and S. Kaucic, J. Phys. (Paris) C **9**, 629 (1987).
[5] C. Can, and C. P. Bhalla, IEEE Trans. Nucl. Sci. **NS-30**, 1090 (1983).
[6] J. L. Campbell, J. A. Maxwell, and W. J. Teesdale, Phys. Rev. C **43**, 1656 (1991).
[7] Y. Isozumi, Nucl. Instrum. Methods A **280**, 151 (1989).
[8] R. L. Intemann, J. Law, and A. Suzuki, J. Phys. (Paris) C **9**, 555 (1987).
[9] A. Suzuki and J. Law, Phys. Rev. C **25**, 2722 (1982).
[10] I. P. Grant, B. J. McKenzie, P. H. Norrington, D. F. Mayers, and N. C. Pyper, Comput. Phys. Commun. **21**, 207 (1980).
[11] M. H. Chen, Phys. Rev. A **31**, 1449 (1985).
[12] M. H. Chen, E. Laiman, B. Crasemann, and H. Mark, Phys. Rev. A **19**, 2253 (1979).
[13] J. B. Mann and W. R. Johnson, Phys. Rev. A **4**, 41 (1971).
[14] I. P. Grant, J. Phys. B **7**, 1458 (1974).
[15] B. J. McKenzie, I. P. Grant, and P. H. Norrington, Comput. Phys. Commun. **21**, 233 (1980).